

Damping of power swings by control of braking resistors

J. Machowski^a, A. Smolarczyk^a, J.W. Bialek^{b,*}

^a*Instytut Elektroenergetyki, Warsaw University of Technology, Koszykowa 75, 00-662 Warsaw, Poland*

^b*School of Engineering, University of Durham, Science Site, South Street, Durham DH1 3LE, UK*

Received 3 February 2000; revised 28 August 2000; accepted 27 October 2000

Abstract

In this paper an analysis of the stability enhancement and improved damping of power swings in a multi-machine power system by means of thyristor-controlled braking resistor installed in the network has been presented. The control law has been derived using direct Lyapunov method and non-linear multi-machine system model. It is optimal in the sense that it causes the quickest dissipation of the power system energy released by a disturbance. Simple implementation of this control using only locally available signal has been also demonstrated. A computer simulation of a multi-machine power system model has verified the effectiveness of the proposed algorithm. © 2001 Elsevier Science Ltd. All rights reserved.

Keywords: Power system stability; Flexible AC transmission systems

1. Introduction

Shunt resistors have been used for stability enhancement of synchronous generators for a long time [1–5]. In early solutions the resistor was switched on using a mechanical switch for a short time (about 0.5 s) after a short circuit close to the generator bus-bars. Then the resistor was switched off and did not take part in the damping of power swings. Its task was simply to increase momentarily the load on the generator in order to brake the accelerating rotor, hence the name *braking resistor* (BR). Recently a rapid growth in high-power electronics resulted in development of a family of thyristor-controlled FACTS devices. By using thyristors the resistor can be either switched on/off or controlled continuously. The thyristor-switched braking resistors (TSBR) and thyristor-controlled braking resistors (TCBR) belong to the family of the FACTS devices [6,7].

Obviously during normal operation of power system both TSBR and TCBR must be switched off. There is also no need to activate them for small disturbances when the system is capable of returning to a stable state by itself. Therefore, a dead-zone must be present to prevent activating the BR when it is not necessary. When (following a large disturbance) the dead-zone limits are exceeded the BR is activated by its controller in order to damp power swings and stabilise the system. In the case of TSBR the bang-bang

control is used and in the case of TCBR the continuous control can be applied.

BR can be installed either in the power plant (with the aim of transient stability improvement and damping of the local power swings) or inside the transmission network (with the purpose to damp the area and inter-area power swings and to improve the dynamic response of the bus-bar voltage).

For BR installed in the power plant the controller can use the speed deviation as the input signal. BR installed inside the transmission network can affect many power plants and its controller can theoretically be based on the state variables of the system (speed deviations and power angles of all generators) or on a locally measurable signal (for example local frequency deviation).

This paper is concerned with a BR installed in the transmission network and deals with the crucial problem of selecting the control law and the controller structure. A wrong control law may not only fail to stabilise the inter-area dynamics, but may also destabilise the system itself [8]. Hence the following questions are posed in the paper:

- What is the optimal control law for TCBR installed in the network, which would provide damping of the power swings due to all generators?
- Is it possible to realise this control law using local measurements only or a centralised control is necessary using a satellite communication system?

The main achievement reported in the paper is that a

* Corresponding author. Tel.: +44-0-191-3743931; fax: +44-0-191-3743838.

E-mail address: janusz.bialek@durham.ac.uk (J.W. Bialek).

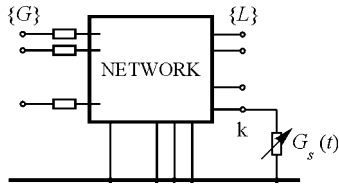


Fig. 1. Schematic illustration of node types.

control law of TCBR providing damping of power swings due to all the generators in the system has been derived using the non-linear model of the multi-machine power system and without resorting to a linearised analysis. As this law requires the knowledge of all state variables (angles, speed deviations and voltages of all the generators), a way of practical implementation of this law by using locally measurable signals has also been discussed.

2. System model

For mathematical derivation of the control algorithm the classical model (constant emf behind the transient reactance) will be used to represent the generators. Power system dynamics are described by the swing equations of the generator rotors:

$$\frac{d\delta_i}{dt} = \Delta\omega_i \quad (1)$$

$$M_i \frac{d\Delta\omega_i}{dt} = P_{mi} - P_i(\delta) - D_i \Delta\omega_i \quad (2)$$

where δ_i and $\Delta\omega_i$ are the rotor angle and the rotor speed deviation, P_{mi} and $P_i(\delta)$ are the electrical and mechanical power, D_i is the damping coefficient and M_i is the inertia coefficient.

The simulations confirming the proposed control algorithm will be performed using a high-order generator model.

All the lines and transformers belonging to the modelled network will be represented by π -equivalent circuits. Power flowing from the transmission to the distribution network will be treated as a load and replaced by constant admittance (included in the equivalent network circuit). All nodes of such network model will be divided (as shown in Fig. 1) into three types:

- {G} — internal generator nodes (behind transient reactance);
- k — the chosen node where BR has been installed;
- {L} — remaining network nodes (mainly load nodes).

In order to analyse the influence of BR on the currents and voltages two cases will be considered, with the BR switched on and the BR switched off.

2.1. Network without BR

The first step in the derivation is to reduce the network model by eliminating nodes {L}. The elimination method is well known — more details can be found in Ref. [5]. The resulting equivalent network connects all the generator nodes {G} and the BR node k and is described by the following nodal admittance equation

$$\begin{matrix} \{G\} \\ k \end{matrix} \begin{bmatrix} \mathbf{I}_G^0 \\ 0 \end{bmatrix} = \begin{bmatrix} \mathbf{Y}_{GG} & \mathbf{Y}_{Gk} \\ \mathbf{Y}_{kG} & Y_{kk} \end{bmatrix} \begin{bmatrix} \mathbf{E}_G \\ V_k^0 \end{bmatrix} \quad (3)$$

where the nodal voltages are $E_i = |E_i| e^{j\delta_i}$ at nodes {G} and $V_k = |V_k| e^{j\theta_k}$ at node k , respectively. The subscripts relate to the sets of nodes. The superscript 0 is added here in order to denote that the relevant quantities relate to the network without BR.

This equivalent network is now reduced by eliminating node k . Resulting network directly connects all the generator nodes {G} and is referred to as the *transfer equivalent network* [5]. It is described by

$$\mathbf{I}_G^0 = \mathbf{Y}_G^0 \mathbf{E}_G \quad (4)$$

$$\mathbf{Y}_G^0 = \mathbf{Y}_{GG} - \mathbf{Y}_{Gk} Y_{kk}^{-1} \mathbf{Y}_{kG} \quad (5)$$

where \mathbf{Y}_G^0 is the square *transfer admittance matrix* for the system without the shunt conductance of BR. The voltage at the BR node is expressed by the following equation

$$V_k^0 = \mathbf{K}_G^0 \mathbf{E}_G \quad (6)$$

$$\mathbf{K}_G^0 = -Y_{kk}^{-1} \mathbf{Y}_{kG} \quad (7)$$

where \mathbf{K}_G^0 is referred to as the *voltage distribution matrix*.

Expanding Eq. (4) for the i th generator gives:

$$I_i^0 = \sum_{j=1}^n Y_{ij} E_j \quad (8)$$

where $Y_{ij} = G_{ij} + jB_{ij}$ are the elements of the admittance matrix determined by Eq. (5) and $E_j = |E_j| e^{j\delta_j}$.

Stability analysis of the multi-machine non-linear system model can be performed by the direct Lyapunov method [5,9]. The total system energy can be used as the Lyapunov function when all the mutual transfer conductances G_{ij} are neglected. The equivalent network is then purely reactive and does not dissipate energy so that, without any external action, the total system energy is constant. Such a model is referred to as *conservative* [5].

When the mutual transfer conductances G_{ij} are neglected, it is necessary to account for the balance of real power by adding shunt conductances, parallel to the shunt conductances representing then loads. With this assumption the generator real power resulting from the emf and current given by Eq. (8) can be expressed as

$$P_i^0 = P_{0i}^0 + \sum_{j=1}^n b_{ij} \sin \delta_{ij} \quad (9)$$

where $b_{ij} = |E_i| |E_j| B_{ij}$ is the magnitude of the power-angle characteristic for the equivalent line connecting a given pair of the generator nodes (i, j) . P_{0i}^0 is the real power of the equivalent load which also contains power losses due to the eliminated mutual transfer conductances G_{ij} . It will be further assumed that P_{0i}^0 is constant, which is an approximation as the power losses do vary during the transient state.

2.2. Network with BR included

BR will be treated as a controlled conductance such that $G_s(t) = P_s(t)/|V_k|^2$, where $P_s(t)$ is the real power absorbed by the resistor, $|V_k|$ is the voltage at the bus-bars where the resistor has been installed.

When a shunt conductance (like BR) is connected to the network, the self-admittance of node k must include the shunt conductance $G_s(t)$. Replacing Y_{kk} in Eqs. (4)–(7) by $[Y_{kk} + G_s]$ gives:

$$\mathbf{I}_G = \mathbf{Y}_G \mathbf{E}_G \tag{10}$$

$$\mathbf{Y}_G = \mathbf{Y}_{GG} - \mathbf{Y}_{Gk} [Y_{kk} + G_s]^{-1} \mathbf{Y}_{kG} \tag{11}$$

$$V_k = \mathbf{K}_G \mathbf{E}_G \tag{12}$$

$$\mathbf{K}_G = -[Y_{kk} + G_s]^{-1} \mathbf{Y}_{kG} \tag{13}$$

The superscript 0 does not appear here because the relevant quantities relate to the network with BR.

All network admittances and electrical quantities depend now on the inverted value of the sum of the shunt conductance G_s and the node self admittance Y_{kk} . This makes Eqs. (10)–(13) very complicated and any direct analysis based on these equations would be very difficult.

In order to simplify Eqs. (10)–(13) note that the admittance Y_{kk} constitutes the short-circuit admittance of the BR node or, in other words, Thevenin's equivalent admittance when looking into node k . Assuming that $G_{kk} \ll B_{kk}$ gives

$$Y_{kk} = G_{kk} + jB_{kk} \cong jB_{kk} = \frac{1}{jX_{SHC}} \tag{14}$$

where $X_{SHC} = -1/B_{kk}$ is the short-circuit reactance (Thevenin's equivalent reactance) of the system at the BR node. Taking into account Eq. (14) it can be written now that

$$\begin{aligned} [Y_{kk} + G_s]^{-1} &= \frac{1}{Y_{kk} + G_s} = \frac{1}{Y_{kk}} \frac{1}{1 + Y_{kk}^{-1} G_s} \\ &\cong Y_{kk}^{-1} \frac{1}{1 + jX_{SHC} G_s} \end{aligned} \tag{15}$$

Note that the short-circuit power is proportional to $1/X_{SHC}$ while the real power of the braking resistor is proportional to $G_s(t)$. For a high-voltage transmission network the short-circuit power varies between a few thousand MVA for weak systems and several thousand MVA for strong systems. The maximum power of the braking resistor is usually between a few tens and a few hundreds MW. Thus

even for weak systems the value of $1/X_{SHC}$ is at least an order of magnitude higher than the value of $G_s(t)$. So it may be assumed that:

$$X_{SHC} G_s \ll 1 \tag{16}$$

Now note that for very small (real or complex) number α such that $|\alpha| \ll 1$ it holds with high accuracy:

$$\frac{1}{(1 + \alpha)} \cong (1 - \alpha) \tag{17}$$

Taking into account Eqs. (17) and (16), Eq. (15) can be written as

$$[Y_{kk} + G_s]^{-1} \cong Y_{kk}^{-1} (1 - jX_{SHC} G_s) \tag{18}$$

On the basis of Eq. (18) the above Eqs. (10)–(13) can be simplified to give

$$\mathbf{Y}_G \cong \mathbf{Y}_G^0 - \Delta \mathbf{Y}_G [-jX_{SHC} G_s] \tag{19}$$

$$\mathbf{I}_G \cong \mathbf{I}_G^0 - \Delta \mathbf{Y}_G \mathbf{E}_G [-jX_{SHC} G_s] \tag{20}$$

$$V_k \cong V_k^0 - Y_{kk}^{-1} \mathbf{Y}_{kG} \mathbf{E}_G [-jX_{SHC} G_s] \tag{21}$$

where

$$\Delta \mathbf{Y}_G = \mathbf{Y}_{Gk} Y_{kk}^{-1} \mathbf{Y}_{kG} \tag{22}$$

I_G^0 , \mathbf{Y}_G^0 , V_k^0 are the corresponding network quantities without the braking resistor given by Eqs. (4)–(7).

Eqs. (19)–(21) show that the influence of the braking resistor on the equivalent network admittances, and therefore on nodal currents and voltages, is additive, i.e. the difference between the values of the network quantities without and with BR is proportional to resistor's conductance.

For the i th generator above Eq. (20) gives

$$I_i \cong I_i^0 - \Delta I_i [-jX_{SHC} G_s] \tag{23}$$

where

$$\Delta I_i = \sum_{j=1}^n \Delta Y_{ij} E_j \tag{24}$$

and I_i^0 is the generator current (Eq. (8)) for the network without BR, ΔY_{ij} are the elements of the matrix given by Eq. (22).

As the current given by Eq. (23) consists of two components, the generator real power corresponding to this current also consists of two components:

$$P_i = P_i^0 - \Delta P_i [X_{SHC} G_s(t)] \tag{25}$$

where P_i^0 corresponds to I_i^0 and ΔP_i corresponds to ΔI_i given by Eq. (24). Note that P_i^0 defines generator's output power without BR connected in the network and is given by Eq. (9). The additional component in Eq. (25) is proportional to ΔP_i and it illustrates the influence of BR on the power of the i th generator.

When the network conductances are neglected, Eq. (22)

gives

$$\Delta Y_{ij} = \frac{jB_{ik}jB_{kj}}{jB_{kk}} = jX_{\text{SHC}}B_{ik}B_{kj} \quad (26)$$

The increment ΔP_i can be calculated from the general formula $\Delta P_i = \text{Re}(E_i \Delta I_i^*)$ by substituting the right-hand side of Eq. (24) for the current increment ΔI_i and then by substituting the right-hand side of Eq. (26) for ΔY_{ij} .

After some trigonometric transformations one gets

$$X_{\text{SHC}} \Delta P_i = -\beta_{ik} \sum_{j=1}^n \beta_{kj} \cos \delta_{ij} \quad (27)$$

where

$$\beta_{ik} = X_{\text{SHC}} B_{ik} |E_i|, \quad \beta_{jk} = X_{\text{SHC}} B_{jk} |E_j| \quad (28)$$

Substituting Eqs. (27) and (9) into Eq. (25) gives:

$$P_i = P_{0i}^0 + \sum_{j=1}^n b_{ij} \sin \delta_{ij} + \left[\beta_{ik} \sum_{j=1}^n \beta_{kj} \cos \delta_{ij} \right] G_s(t) \quad (29)$$

where P_{0i}^0 is the real power of the equivalent load defined in Eq. (9).

The coefficient β_{jk} defined in Eq. (28) constitutes an electrical measure of the distance between the generator internal nodes $i \in \{G\}$ and the BR node k .

Note that the third component in Eq. (29), representing the influence of BR, does depend on *cosinus* of power angles. The second (and main) component in this equation depends on *sinus* of power angles.

2.3. Conservative model of the power system

A simplified power system model resulting from Eqs. (1), (2) and (29) can be summarised in the following set of state–space equations

$$\frac{d\delta_i}{dt} = \Delta \omega_i \quad (30)$$

$$\begin{aligned} \frac{d\Delta \omega_i}{dt} = & \frac{1}{M_i} [P_{mi} - P_{0i}^0] - \frac{1}{M_i} \sum_{j=1}^n b_{ij} \sin \delta_{ij} - \frac{D_i}{M_i} \Delta \omega_i \\ & - \frac{1}{M_i} \left[\beta_{ik} \sum_{j=1}^n \beta_{kj} \cos \delta_{ij} \right] G_s(t) \end{aligned} \quad (31)$$

No energy is dissipated in the transmission network because the power losses in the transfer mutual conductances have been added to the equivalent loads as constant values. In this conservative model energy is dissipated only by the natural damping torque of the generators (the third component on the right-hand side of Eq. (31)) and by the influence of the controlled braking resistor (the last component on the right-hand side of Eq. (31)).

3. Optimal control

The main question to be answered now is how $G_s(t)$ should be controlled so that the strongest damping of rotor swings in the system is achieved. As the BR can be located anywhere in the network, it can influence many generators. Hence the words ‘strongest damping’ should refer to the system as the whole rather than individual generators. In this context a question arises as to what is the measure of damping for the system as the whole. The answer to this question will be provided by Lyapunov’s direct method.

3.1. Lyapunov’s direct method

The kinetic and potential energy of the considered conservative power system model corresponds to the integrals of the first and second component of the swing equation (31)

$$E_K = \sum_{i=1}^n \int_0^{\omega_i} M_i \Delta \omega_i d\Delta \omega_i = \frac{1}{2} \sum_{i=1}^n M_i \Delta \omega_i^2 \quad (32)$$

$$\begin{aligned} E_P = & - \sum_{i=1}^n \int_{\delta_i^s}^{\delta_i} \left[(P_{mi} - P_{0i}^0) - \sum_{j=1}^n b_{ij} \sin \delta_{ij} \right] d\delta_i \\ = & \sum_{i=1}^n (P_{mi} - P_{0i}^0) (\delta_i - \delta_i^s) - \sum_{i=1}^{n-1} \sum_{j>i}^n b_{ij} [\cos \delta_{ij} - \cos \delta_{ij}^s] \end{aligned} \quad (33)$$

where δ_i^s is the power angle of the post-fault stable equilibrium point. The total system energy is equal to the sum of the kinetic and potential energy:

$$V(\delta, \Delta \omega) = E_K + E_P \quad (34)$$

It can be shown [5,9] that this function is positive-definite. For the system without controlled resistor the time derivative $\dot{V} = dV/dt$ along the system trajectory is negative semi-definite. Whether or not \dot{V} is negative for the system with controlled resistor and how big is this derivative depends on the chosen control law of $G_s(t)$.

3.2. Control law

Any disturbance in the system involves a power imbalance that moves the system trajectory from the pre-fault stable equilibrium point to a transient point that has a higher energy level than the post-fault equilibrium point. The speed with which the system returns to an equilibrium point is therefore the measure of the system damping. This speed is given by the rate of change $\dot{V} = dV/dt$, which defines the speed with which the energy released by the disturbance is dissipated.

Thus a given control law is optimal in the Lyapunov sense if it maximises the negative value of the time derivative \dot{V} . Obviously such law is optimal only for a particular Lyapunov function. As Lyapunov functions are non-unique,

another definition of the Lyapunov function may result in a different control law.

The overall methodology used to derive the optimal control law, as described below, has been applied previously by the same authors to the shunt compensators [10], SMES [11], series compensator [12] and the PSS [13–15].

The time derivative \dot{V} along any system trajectory can be expressed:

$$\begin{aligned} \dot{V} &= \frac{dV}{dt} = \frac{dE_K}{dt} + \frac{dE_P}{dt} \\ &= \sum_{i=1}^n \frac{\partial E_K}{\partial \Delta\omega_i} \frac{d\Delta\omega_i}{dt} + \sum_{i=1}^n \frac{\partial E_P}{\partial \delta_i} \frac{d\delta_i}{dt} \end{aligned} \quad (35)$$

Differentiating Eqs. (32) and (33) gives:

$$\frac{\partial E_K}{\partial \omega_i} = M_i \Delta\omega_i \quad (36)$$

$$\frac{\partial E_P}{\partial \delta_i} = -(P_{mi} - P_{0i}^0) - \sum_{j \neq i}^n b_{ij} \sin \delta_{ij}$$

After substituting Eq. (36) into Eq. (35) and taking into account Eqs. (30) and (31) one gets:

$$\dot{V} = \frac{dV}{dt} = \frac{dE_K}{dt} + \frac{dE_P}{dt} = - \sum_{i=1}^n D_i \Delta\omega_i^2 - \dot{V}_s \quad (37)$$

where

$$\dot{V}_s = - \left[\sum_{i=1}^n \Delta\omega_i \beta_{ik} \sum_{j=1}^n \beta_{kj} \cos \delta_{ij} \right] G_s(t) \quad (38)$$

and $\Delta\omega_i = d\delta_i/dt$.

Eqs. (37) and (38) determine by how much the control of BR can influence the dissipation of energy in the system. Thus the control law for $G_s(t)$ should ensure that \dot{V}_s is always negative and has as high as possible value. This can be achieved using the following control law:

$$G_s(t) = K \sum_{i=1}^n \Delta\omega_i \beta_{ik} \sum_{j=1}^n \beta_{kj} \cos \delta_{ij} \quad (39)$$

where K is controller's gain. This control law results in

$$\dot{V}_s = -K \left[\sum_{i=1}^n \Delta\omega_i \beta_{ik} \sum_{j=1}^n \beta_{kj} \cos \delta_{ij} \right]^2 < 0 \quad (40)$$

which means that the control law ensures energy dissipation at any instant of time.

It is informative to compare the control law (39) with a well-known simple rule resulting from the generator-infinite bus-bar system. As damping is proportional to the speed deviation, using the control law $G_s(t) = K\Delta\omega$ will provide additional damping in such a simple system [5]. To execute this control law the shunt element conductance $G(t)$ must change its sign at the instants when the speed deviation changes the sign. These are so called switching points.

The situation is not so simple in a multi-machine system when some generators swing against each other or their swings are not in the phase. The signs of individual speed deviations $\Delta\omega_i$ (for $i = 1, \dots, n$) do not change at the same time. Generally there may be no time intervals for which all $\Delta\omega_i$ have the same sign. Hence, taking only the sign of $\Delta\omega_i$ (for $i = 1, \dots, n$), it is impossible to find time intervals for which the resistor should be switched on.

The optimal control law derived in this paper takes into account not only the sign of individual $\Delta\omega_i$ but also their influence as expressed by coefficients β_{ik}, β_{kj} . Consequently the sign and value of $G_s(t)$ are determined by the closest (large β_{ik}, β_{kj}) and most heavily swinging generators (large $\Delta\omega_i$). Such a choice of the sign and value of $G_s(t)$ is optimal from the point of view of the whole system as it ensures monotonic dissipation of energy released by a disturbance. Note however that such control may cause a temporary enhancement of swings of some of the less swinging generators (small $\Delta\omega_i$) or those further away from the resistor (small β_{ik}, β_{kj}). This means that the control law (39) is optimal from the system point of view, but not necessarily from the point of view of individual generators.

Obviously when there is more than one controlled element (such as TCBR) in the system, then it is possible to damp simultaneously the swings due many more generators and the overall damping is much faster. However the control of a single element must always be based on a compromise between the demands of all the generators, i.e. $G_s(t)$ should be chosen such that the damping is strongest for the closest and most heavily swinging generators.

As $(\Delta\omega_i, \delta_i)$ are the state variables of the system, Eq. (39) describes a state-variable control. Such control could be executed by a central computer, which would identify the dynamic state of the system using, e.g. a satellite communication system. The authors of this paper do not recommend such a solution due to a high cost and reliability problems connected with employing a satellite communication system. The next section shows how the state-variable control can be executed using only locally measurable signals.

4. Control based on local signal

For practical implementation the control based on Eq. (39) must be replaced by a control utilising only locally measurable signal. How exactly such local control will emulate the optimal state-variable control depends on the choice of the signal and the structure of the controller. The choice of the suitable signal will be now discussed.

4.1. Properties of signals

Let q_G denotes a quantity, which can be measured locally at the BR node. In the steady-state each electrical quantity in the transmission network depends on power flows and therefore on the power angles δ_i . Hence (assuming constant

magnitude of the electromotive forces) the time derivative of q_G can be expressed as:

$$\frac{dq_G}{dt} = \frac{\partial q_G}{\partial G_s} \frac{dG_s}{dt} + \sum_{i=1}^n \Delta\omega_i \frac{\partial q_G}{\partial \delta_i} \quad (41)$$

where $\Delta\omega_i = d\delta_i/dt$.

The first component on the right-hand side of Eq. (41) relates to the sensitivity of q_G to the changes in $G_s(t)$. If this sensitivity $\partial q_G/\partial G_s$ is small, this component can be neglected and Eq. (41) simplifies to:

$$\sum_{i=1}^n \Delta\omega_i \frac{\partial q_G}{\partial \delta_i} \cong \frac{dq_G}{dt} \quad (42)$$

The left-hand side of Eq. (42) depends on speed deviations $\Delta\omega_i$ and is the same as in the optimal control law (39) if the following condition is satisfied:

$$\frac{\partial q_G}{\partial \delta_i} = \beta_{ik} \sum_{j=1}^n \beta_{kj} \cos \delta_{ij} \quad (43)$$

This simplifies the state-variable control (39) to:

$$G_s(t) \cong K \frac{dq_G}{dt} \quad (44)$$

Now it will be shown that condition (43) is satisfied by the signal q_G corresponding to the phase angle θ_k of the voltage at the BR node.

4.2. Choice of the signal

Voltage at the BR node is given by Eq. (21). For the conservative system model Eq. (21) gives:

$$V_k \cong \varphi(G_s)\varphi(\delta) \quad (45)$$

where

$$\varphi(G_s) = 1 - jX_{SHC}G_s \quad (46)$$

$$\begin{aligned} \varphi(\delta) &= -B_{kk}^{-1} \mathbf{B}_{kG} \mathbf{E}_G = -\sum_{j=1}^n B_{kk}^{-1} B_{kj} |E_j| e^{j\delta_j} \\ &= -\sum_{j=1}^n \beta_{kj} [\cos \delta_j + j \sin \delta_j] \end{aligned} \quad (47)$$

Taking into account Eq. (16) and neglecting the very small value of $X_{SHC}G_s$, the above Eqs. (46) and (45) can be simplified to:

$$\varphi(G_s) \cong 1, \quad \varphi(\delta) \cong V_k \quad (48)$$

Eqs. (47) and (48) now give:

$$V_k = |V_k| e^{j\theta_k} \cong \varphi(\delta) = -\sum_{j=1}^n \beta_{kj} [\cos \delta_j + j \sin \delta_j] \quad (49)$$

Let θ_k be the voltage phase angle. Eq. (49) then gives:

$$|V_k| \cos \theta_k = -\sum_{j=1}^n \beta_{kj} \cos \delta_j \quad (50)$$

$$|V_k| \sin \theta_k = -\sum_{j=1}^n \beta_{kj} \sin \delta_j \quad (51)$$

Hence

$$\tan \theta_k \cong \frac{\sum_{j=1}^n \beta_{kj} \sin \delta_j}{\sum_{j=1}^n \beta_{kj} \cos \delta_j} \quad (52)$$

$$|V_k|^2 = \left[\sum_{j=1}^n \beta_{kj} \sin \delta_j \right]^2 + \left[\sum_{j=1}^n \beta_{kj} \cos \delta_j \right]^2 \quad (53)$$

Applying the chain rule to Eqs. (52) and (53) gives:

$$\begin{aligned} |V_k|^2 \frac{\partial \theta_k}{\partial \delta_i} &= \beta_{ki} \cos \delta_i \sum_{j=1}^n \beta_{kj} \cos \delta_j + \beta_{ki} \sin \delta_i \sum_{j=1}^n \beta_{kj} \sin \delta_j \\ &= \beta_{ki} \sum_{j=1}^n \beta_{kj} [\cos \delta_i \cos \delta_j + \sin \delta_i \sin \delta_j] \end{aligned} \quad (54)$$

and finally (taking into account that $\beta_{ki} = \beta_{ik}$):

$$|V_k|^2 \frac{\partial \theta_k}{\partial \delta_i} = \beta_{ik} \sum_{j=1}^n \beta_{kj} \cos \delta_{ij} \quad (55)$$

Now it should be noticed that for the considered system model the time derivative of the phase angle $d\theta_k/dt$ is proportional to the local frequency deviation Δf_k measured at the BR node: $\Delta f_k = ((1/(2\pi)) d\theta_k)/dt$. A signal proportional to the squared voltage $|V_k|^2$ multiplied by the local frequency deviation Δf_k can be therefore expressed as:

$$K_{\Delta f} |V_k|^2 \Delta f_k = K |V_k|^2 \frac{d\theta_k}{dt} \cong K |V_k|^2 \sum_{i=1}^n \frac{\partial \theta_k}{\partial \delta_i} \frac{d\delta_i}{dt} \quad (56)$$

where $K_{\Delta f} = K/2\pi$. Taking into (55) and $d\delta_i/dt = \Delta\omega_i$ one can obtain from Eq. (56) that:

$$K_{\Delta f} |V_k|^2 \Delta f_k = K \sum_{i=1}^n \Delta\omega_i \beta_{ik} \sum_{j=1}^n \beta_{kj} \cos \delta_{ij} \quad (57)$$

The right-hand-side of Eq. (57) is the same as the right-hand-side of Eq. (39). Hence the state-variable control (39) can be replaced by:

$$G_s(t) = K_{\Delta f} |V_k|^2 \Delta f_k(t) \quad (58)$$

In this equation the multiplication of the gain $K_{\Delta f}$ by $|V_k|^2$ has the effect of gain tuning. From the point of view of the dynamic response of the voltage at the BR node, such tuning is profitable. When $|V_k|$ decreases significantly during the

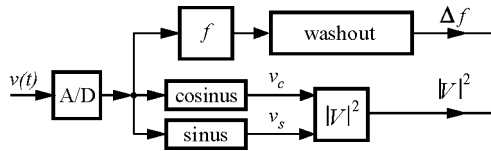


Fig. 2. Simplified block diagram of measuring element.

transient state, multiplication by $|V_k|^2$ reduces the effective gain and does not allow the controller to force a high value of $G_s(t)$ which could further decrease the voltage. On the other hand when $|V_k|$ increases during the transient state, multiplication by $|V_k|^2$ increases the effective gain and forces a higher value of $G_s(t)$ that improves both power system damping and the dynamic voltage response.

It should be emphasised that the control law (58) emulates the optimal control law (39) only with certain accuracy determined by approximated assumptions, the most important of which is neglecting the sensitivity $\partial q_G / \partial G_s$ of given signal to the changes of $G_s(t)$. If this sensitivity is not neglected then an additional component would appear in Eq. (58) compensating for the changes of Δf_k due to changes in $G_s(t)$. In the block diagram of the controller, such compensating component would correspond to a feedback loop of a differentiating type. The question of neglecting the sensitivity $\partial q_G / \partial G_s$ was the subject of simulation studies and will be discussed in the next section.

Application of Δf_k as the input signal for the BR controller is not new and has already been reported in many papers. For example Ref. [6] recommends the use of a proportional controller fed by the frequency deviation while Ref. [8] recommends the use of a PID controller.

It should be emphasised that it was not the aim of this paper to show yet again that Δf_k could be used as the input

signal. What we consider our achievement is that we have proved that using Δf_k as the feedback signal damps the power swings in the multi-machine system as the whole and can approximately emulate the optimal state-variable control resulting from the direct Lyapunov method. And the important thing is that we have used the non-linear system model without resorting to linearisation. This has important consequences for the robustness of the stabiliser.

4.3. Block diagram of the controller

A controller of BR must consist of two parts: (a) element measuring the signals Δf_k , $|V_k|^2$; and (b) regulator of $G_s(t)$ with a supplementary loop producing a stabilising signal proportional to signal given by Eq. (58).

There is a number of algorithms allowing to determine digitally the voltage magnitude and frequency or frequency deviation [16–19]. They differ with the speed of dynamic response and ability to filter out harmonics appearing in the input signal.

For the proposed control the measuring algorithm does not need to be very fast but it should possess good filtering properties such that the output signal is smooth during the swings. Fig. 2 shows the block diagram of a measuring element where the squared voltage magnitude $|V_k|^2$ is calculated by decomposition of the voltage signal into two orthogonal signals by using orthogonal functions *sinus* and *cosinus*. Frequency f is measured by the zero-crossing method and the frequency deviation Δf is obtained using a washout element.

The transfer function and the parameters of the washout element have to be chosen in such a way that the following conditions are satisfied. The Bode magnitude plot must start at zero frequency in order that the element does not pass through any constant signals. Within the swing frequency range (0.2–2 Hz), the signals must be passed by the element with approximately the unity gain and with the smallest possible phase shift. Typically such washout element consists of one differentiating element and two lead-lag elements. Fig. 3 shows the block diagram of such washout element and its frequency characteristic for sample parameters: $K_w = 1.5$, $T_w = 10$, $T_1 = 0.05$, $T_2 = 0.02$, $T_3 = 3$, $T_4 = 5.4$.

Measured signals Δf , $|V_k|^2$ are used as the input signals of the supplementary loop of the regulator shown in Fig. 4. The lower part consists of an integral regulator with negative feedback. This part of the regulator forces $G_s(t)$ to settle down at the reference value $G_{ref} = 0$. Thanks to that the BR is not activated during normal operation or an abnormal state with a permanent frequency deviation. The supplementary loop (upper part of the diagram) forces the stabilising signal as defined by Eq. (58). This part has the dead zone for Δf in order to avoid unnecessary acting of BR during small disturbances in the system.

The output signal of the regulator is passed through a

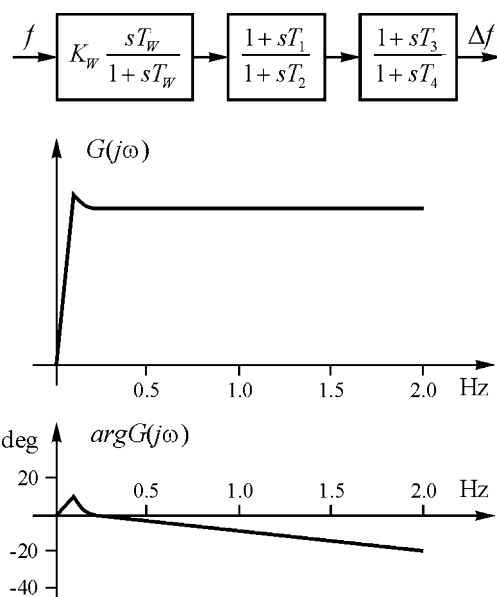


Fig. 3. Block diagram of the washout element and its frequency characteristics.

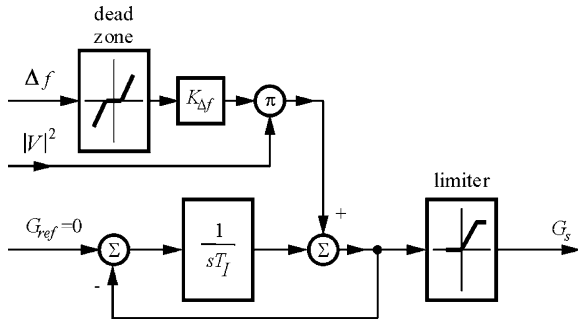


Fig. 4. Block diagram of the BR regulator.

limiter. As $G_s(t)$ can be only positive, the output limiter passes through only the positive part of the control signal.

Note that the feedback signal of the integrator (lower part of the diagram) is taken from the input of the limiter, so that it takes both positive and negative values. For a large integration time constant ($T_I \approx 10\text{--}20$ s), much larger than the period of the power swings, the integral of the feedback signal is close to zero as the positive and negative parts of the signal cancel each other out. Consequently the integrator practically does not influence controller's output signal. It acts only when there is a permanent frequency deviation in the system in a new post-fault equilibrium point.

5. Simulation results

The effectiveness of the proposed control law will be now illustrated using a 3-machine sample system shown in Fig. 5. Each synchronous generator has been modelled by the sixth-order model [5].

The parameters of this sample system have been chosen in such a way that one generator G3 is large and corresponds to a system (infinite bus-bar). The inertia coefficient of generator G2 is much smaller than that of generator G1. Therefore the swings of generator G2 are little faster (with respect to G3) than those of G1. A disturbance inside the network causes both generators G1 and G2 to swing and the swings due to these two different frequencies are superimposed on each other causing distortions in the measuring signals. This is similar to the swings in a real system, where the swings inside the network (resulting from many generators) are multi-modal.

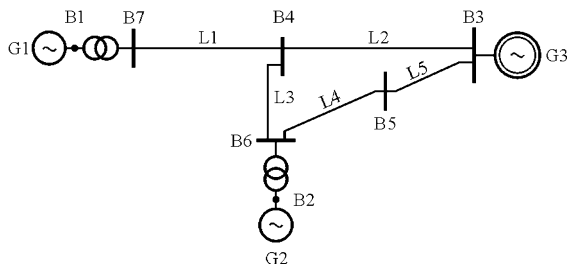


Fig. 5. The three-machine test system.

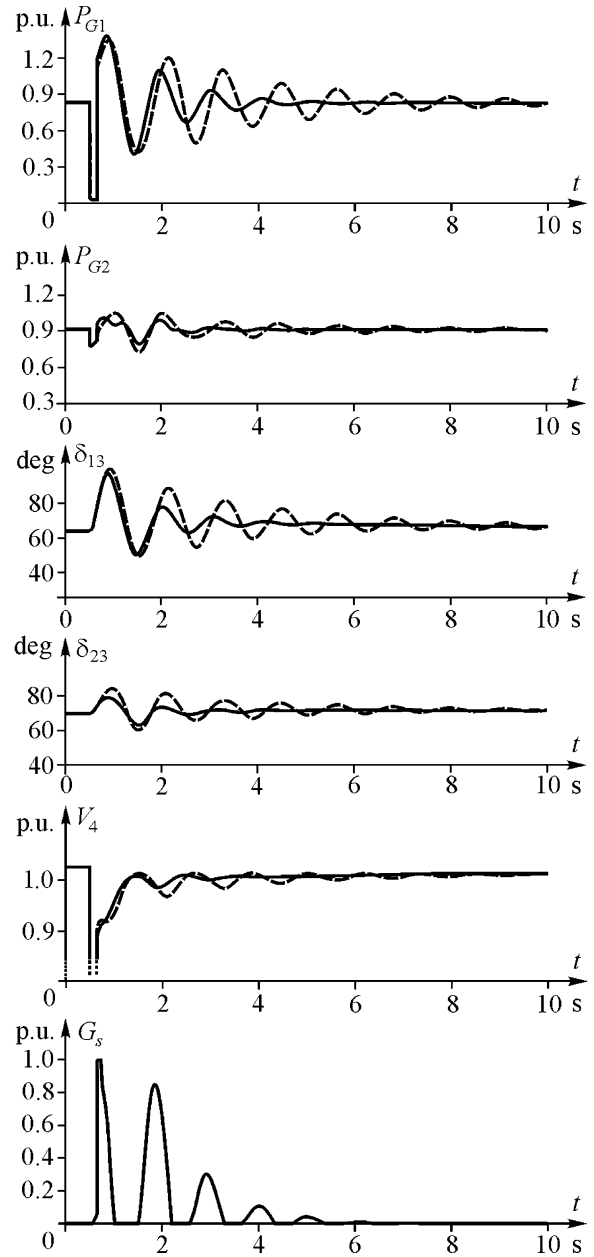


Fig. 6. Simulation results for a temporary fault at node B7 without braking resistors (dashed line) and when TCBR is installed at node B4 (solid line).

Faults were simulated in each node and, for each fault, different locations of BR were studied. An example of simulation results, for a resistor located inside the network at node B4 is shown in Fig. 6. Proposed controller stabilises the power and angle oscillations quite well. As node B4 is far away from both the generators, G1 and G2, the first swing is not very well damped. However the second and the third swing are damped far better and the settling time is far shorter than without BR.

It is interesting to observe the dynamics of the voltage at the BR node. It is well known that often a stabiliser, which damps well power swings, deteriorates the dynamic voltage response. Fig. 6 shows that the proposed stabiliser does not

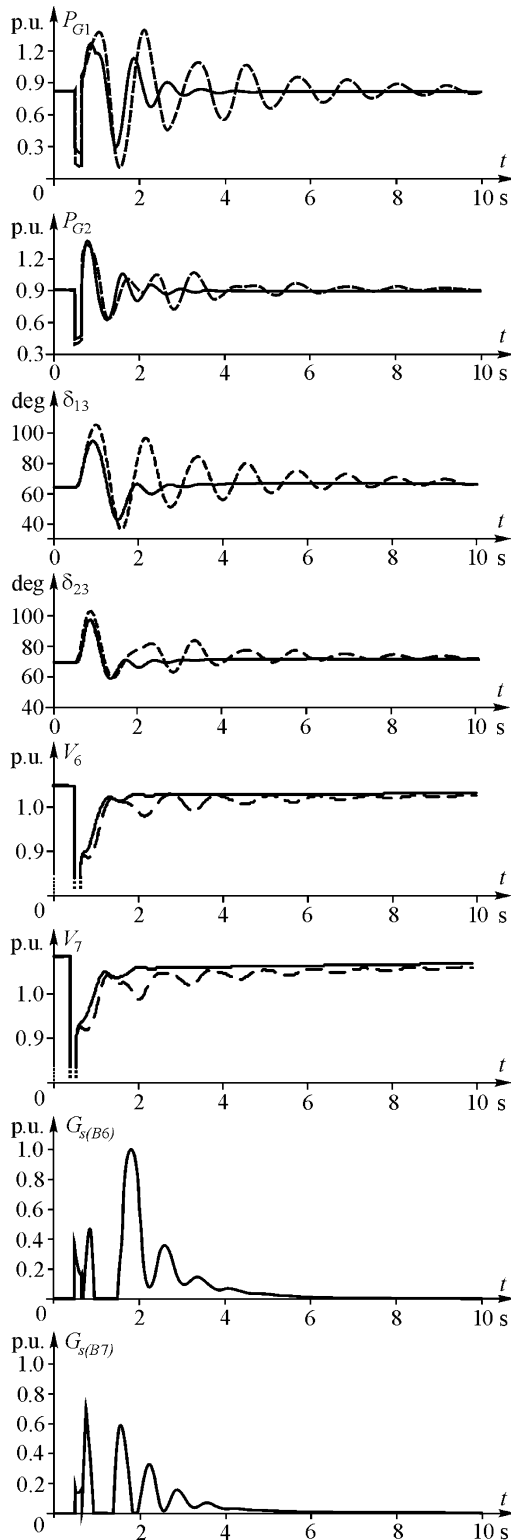


Fig. 7. Simulation results for a temporary fault at node B4 without BR (dashed line) and when BR were installed at nodes B6 and B7 (solid line).

suffer from this weakness and that the voltage response is even slightly improved when compared to the case without BR.

Fig. 7 shows an example of simulation results when two

TCBRs are installed at the generator nodes B6 and B7. Obviously in this case the proposed control resulted in a strong damping of power swings. Also the voltage response was improved.

Simulation studies included verification of Eq. (42), i.e. the influence of neglecting the sensitivity $\partial q_G/\partial G_s$. The sensitivity coefficient of the phase angle $\partial \theta_k/\partial G_s$, or the local frequency deviation $\partial \Delta f_k/\partial G_s$, is negative because the phase angle and the frequency decrease when the BR conductance is increased. Compensation of this negative sensitivity requires the use of a ‘positive’ feedback loop, which adversely influences stability of the control system and reduces gain K of the supplementary control loop. It has been also found that this ‘positive’ feedback loop does not improve significantly the damping resulting from TCBR. This confirms the validity of neglecting $\partial q_G/\partial G_s$, in Eq. (41).

In the case shown in Fig. 6, when the BR is installed in node B4, the sensitivity coefficient of the phase angle was approximately equal to $\partial \theta_k/\partial G_s \cong 0.047$ p.u. The first component in Eq. (41), corresponding to $(\partial \theta_k/\partial G_s) (dG_s/dt)$ and omitted in Eq. (42), did not exceed 20% of the value of the second, not omitted in Eq. (42), component of Eq. (41) corresponding to $\sum_{i=1}^n \Delta \omega_i (\partial \theta_k/\partial \delta_i)$.

It is also interesting to compare the optimal control (39), based on the state variables, with its emulation by a local controller (58) using the frequency deviation. The tests have shown that the state-variable control is very robust indeed with a very smooth operation even for a very high gain K . The local controller, although far simpler and easier to implement, provides worse damping than the centralised state-variable controller. There are two main reasons for this. Firstly the equality between the right-hand side of Eq. (57) and the right-hand side of Eq. (39) is only within the accuracy of adopted assumptions. Secondly a disturbance may cause large jumps in the value of electrical quantities measured in the network and these jumps may disturb the measurement of the quantities. Hence the measuring elements must possess good filtering properties which obviously affect adversely the dynamic response of the controller.

6. Summary

Traditionally braking resistors have been used at power stations to improve transient stability. The recent progress in power electronics allows using the thyristor-switched (TSBR) and thyristor-controlled braking resistors (TCBR). Such devices can be installed at a location inside the network with the purpose to damp the area and inter-area power swings and to improve the dynamic voltage response. In such a case the challenge is to derive a control law which would damp power swings due to all the generators. This paper has presented theoretical analysis of this problem using the non-linear multi-machine system model and the direct Lyapunov’s method. The control law was initially

derived using the system state variables such as rotor angles and rotor speed deviations as the input variables. Then it was shown that the law does not require using complicated and expansive satellite communication systems but can be implemented using a simple controller employing only locally available variables such as the square voltage magnitude and the frequency deviation. The theory and the implementation of the proposed stabilising controller has been finally verified by simulation using a simple multi-machine test system.

References

- [1] Shelton ML, Winkelman RF, Mittelstadt WA, Bellerby WL. Bonneville power administration 1400 MW braking resistor. *IEEE Trans PAS* 1975;94:602–11.
- [2] Grobovoy AA, Lizalek NN. Multiple dynamic brake and power system emergency control. *Powercon'98*, Beijing, China, 18–21 August 1998.
- [3] CIGRE SC38-WG02 Report State of Art. Non-classical means to improve power system stability. *Electra*, No. 118, May 1998.
- [4] Kundur P. *Power system stability and control*. New York: McGraw-Hill, 1994.
- [5] Machowski J, Bialek J, Bumby J. *Power system dynamics and stability*. New York: Wiley, 1997.
- [6] Carlson DL, Maki DS. Feasibility study for application of thyristor controlled braking resistor (TCBR) on the Northern MAPP transmission system. *FACTS applications*, IEEE Catalogue Number: 96TP 116-0, chap. 8.5.
- [7] Modeling of power electronics equipment (FACTS) in load flow and stability programs. *CIGRE Task Force 38.01.08*, August 1999.
- [8] Nonlinear control and operation of methodologies and basic concepts, *FACTS*. EPRI Report TR 103398, February 1995.
- [9] Pai MA. *Energy function analysis for power system stability*. Dordrecht: Kluwer Academic, 1989.
- [10] Machowski J, Nelles D. Power system transient stability enhancement by optimal control of static VAR compensators. *Int J Electl Power Energy Syst* 1992;14(6):411–21.
- [11] Machowski J, Nelles D. Optimal modulation controller for superconducting magnetic energy storage. *Int J Electl Power Energy Syst* 1994;16(5):291–300.
- [12] Machowski J, Robak S, Bialek J. Damping of power swings by optimal control of series compensators. *Proceedings of the 10th International Conference on Power System Automation and Control*, Bled, Slovenia, October 1997. p. 39–4.
- [13] Machowski J, Robak S, Bialek W, Bumby J. Decentralized damping of Power Swings-Feasibility Study. EPRI (Palo Alto, USA), Report TR-112417.
- [14] Machowski J, Robak S, Bialek JW, Bumby JR. A novel excitation control system for use with synchronous generators. *IEEE Proc Gener Transm Distrib* 1998;145(5):537–46.
- [15] Machowski J, Robak S, Bialek JW, Bumby JR, Abi-Samra N. Decentralized stability-enhancing control of synchronous generator. *IEEE paper PE-007PRS (04-2000)*.
- [16] Phadke AG, Thorap JS, Adamiak MG, new measurement technique for tracking voltage phasors, local system frequency and rate of change of frequency. *IEEE Trans PAS* 1983;102(5):1025–38.
- [17] Giris AA, Peterson WL. Adaptive estimation of power system frequency deviation and its rate of change for calculating sudden power system overloads. *IEEE Trans PWDR* 1990;5(2):585–94.
- [18] Kamwa I, Grondin R. Fast adaptive scheme for tracking voltage phasor and local frequency in power transmission and distribution systems. *IEEE Trans PWRD* 1992;7(2):789–95.
- [19] Denis Ph, Counan C, Hossenlopp L, Holweck C. Measurement of voltage phase for the french future defence plan against losses of synchronism. *IEEE Trans Power Delivery* 1992;7:62–69.